DALTON
FULL PAPER

# A new 3-D polymeric spin transition compound: [tris(1,4-bis-(tetrazol-1-yl)butane-*N*1,*N*1′)iron(II)] bis(perchlorate)

**Petra J. van Koningsbruggen,*[ad] Yann Garcia,*[ad] Huub Kooijman,[b] Anthony L. Spek,†[b] Jaap G. Haasnoot,[c] Olivier Kahn,[d] Jorge Linares,[e] Epiphane Codjovi[de] and François Varret*[e]**

[a] *Institut für Anorganische Chemie und Analytische Chemie, Johannes-Gutenberg Universität, Staudingerweg 9, 55099 Mainz, Germany. E-mail: garcia@iacgu7.chemie.uni-mainz.de*
[b] *Bijvoet Center for Biomolecular Research, Crystal and Structural Chemistry, Utrecht University, Padualaan 8, 3584 CH Utrecht, The Netherlands*
[c] *Leiden Institute of Chemistry, Gorlaeus Laboratories, Leiden University, PO Box 9502, 2300 RA Leiden, The Netherlands*
[d] *Institut de Chimie de la Matière Condensée de Bordeaux, Av. du Dr. A. Schweitzer, 33608 Pessac Cedex, France*
[e] *Laboratoire de Magnétisme et d'Optique CNRS - Université de Versailles, UMR 8634, 45 Av. des Etats-Unis, 78035 Versailles Cedex, France. E-mail: fvarret@physique.uvsq.fr*

***Received 5th October 2000, Accepted 5th December 2000***
***First published as an Advance Article on the web 29th January 2001***

A series of novel polymeric compounds of formula $[M(btzb)_3][ClO_4]_2$ ($M^{II}$ = Fe, Ni or Cu) with btzb = 1,4-bis-(tetrazol-1-yl)butane have been prepared and their physical properties investigated. The btzb ligand has been prepared and its crystal structure determined, together with a tentative crystal structure of the 3-D compound $[Fe(btzb)_3][ClO_4]_2$. The model of the latter shows two symmetry-related, interpenetrating Fe–btzb networks in which the iron(II) ions approach each other as close as 8.3 and 9.1 Å. This supramolecular catenane undergoes a sharp thermal spin transition around 160 K with hysteresis (20 K) along with a pronounced thermochromic effect. The spin crossover behaviour has been followed by magnetic, DSC, optical spectroscopy and $^{57}$Fe Mössbauer spectroscopy measurements. Irradiation with green light at low temperature leads to population of the metastable high-spin state for the thermally active iron(II) ions. The nature of the spin crossover behaviour has been discussed in detail.

## Introduction

The fast developments in advanced electronic technology require compounds showing a bistability behaviour on the molecular scale.[1] A fascinating example of molecular bistability is represented by iron(II) spin crossover (SC) compounds, which show a transition from the high-spin state (HS, $S = 2$) to the low-spin state (LS, $S = 0$) on cooling, upon increasing pressure, or by light irradiation.[2–10] The use of such materials as molecular-based memory devices and displays is currently investigated.[9,11,12]

It is well accepted that the driving force for the SC process is the gain in entropy, which is predominantly vibrational in origin. Therefore, it may be proposed that in polynuclear systems the molecular distortions involved in the LS to HS transition may efficiently be spread throughout the whole crystal lattice *via* the ligands linking the SC centres. This led us to design new ligands of the bis(tetrazole) type, with which the first structurally characterised 1-D iron(II) SC compound has recently been reported.[13] [Tris(1,2-bis(tetrazol-1-yl)propane)-iron(II) bisperchlorate shows a gradual SC behaviour with transition temperature $T_{1/2}$, *i.e.* where equivalent amounts of $Fe^{II}$ in LS and HS forms are present, of 148 K. The single-crystal structure determination was carried out above (200 K) and below (100 K) the transition temperature. The molecular structure consists of a 1-D chain in which the iron(II) ions are linked by three *N*4,*N*4′ coordinating bis(tetrazole) ligands. The main difference between the two forms appears to be in the Fe–N distances, which are 2.164(4) Å at 200 K and 2.038(4) Å at 100 K. The Fe···Fe separations decrease upon cooling from 7.422(1) (200) to 7.273(1) Å (100 K). Continuing our strategy of applying the linkage of tetrazole moieties by alkyl groups in order to obtain polynuclear iron(II) SC materials, we decided to vary the length of the alkyl spacer. In this way we envisaged a study of the effect of the increase in the Fe···Fe separation on the SC properties. In this paper we report on the crystal structure of 1,4-bis(tetrazol-1-yl)butane (abbreviated as btzb), as well as on the physical properties of the polynuclear compounds $[M(btzb)_3][ClO_4]_2$ ($M^{II}$ = Fe, Ni or Cu). A tentative model for the 3-D structure of $[Fe(btzb)_3][ClO_4]_2$ is also presented.

## Experimental

Infrared spectra were recorded out with a Perkin-Elmer Paragon 1000 FT-IR spectrophotometer using KBr pellets, UV/Visible spectra with a CARY 5E spectrophotometer using the diffuse reflectance technique, with polytetrafluoroethylene as a reference. Magnetic susceptibilities were measured in the temperature range 300–5 K with a fully automated Manics DSM-8 susceptometer equipped with a TBT continuous-flow cryostat and a Drusch EAF 16 UE electromagnet operating at *ca.* 1.7 Tesla. LIESST (Light-Induced Excited Spin State Trapping) experiments were carried out using a $Kr^+$ laser ($\lambda = 514$ nm) coupled through an optical fibre to the cavity of a Quantum Design MPMS-5S SQUID magnetometer. Magnetic data were corrected for diamagnetic contributions, which were estimated from the Pascal constants. X-Band powder EPR spectra were obtained on a Bruker ESP 300 E electron spin resonance spectrometer. $^{57}$Fe Mössbauer

† For enquiries related to crystallographic studies.

 DOI: 10.1039/b008073j

measurements were obtained on a constant acceleration conventional spectrometer with a room temperature $^{57}Co$ source (rhodium matrix) in transmission geometry. Isomer shifts are given with respect to metallic Fe at room temperature. The spectra were fitted by the sum of lorentzians in a least-squares refinement. Variable temperature optical data monitoring the iron(II) spin transition at 520 nm were recorded on a home-made device.[8,14] The DSC experiments were performed with a Perkin-Elmer DSC-7 instrument working down to 100 K. Details of the experimental procedure are given elsewhere.[15] The sweep rate was fixed at 5 K $min^{-1}$. Reagents were commercially available and not purified further.

### Syntheses

**1,4-Bis(tetrazol-1-yl)butane (btzb).** The ligand btzb has been prepared according to a modification of the general method of Kamiya and Saito.[16] A mixture of 1,4-diaminobutane (1.76 g, 0.02 mmol) and sodium azide (3 g, 0.04 mmol) in 30 g of triethyl orthoformate and 40 ml of acetic acid was stirred and heated to 75 °C for 3 hours. The resulting solution was evaporated to dryness and the residue subsequently dissolved in water, whereby the inorganic salts dissolved and the required product remained as a white precipitate. It was filtered off and washed with water. Recrystallisation from methanol yielded plate-shaped single crystals. Yield: 1.88 g, 48% (Calc. for $C_6H_{10}N_8$: C, 37.11; H, 5.19; N, 57.70. Found: C, 36.91; H, 5.27; N, 57.16%).

**$[Fe(btzb)_3][ClO_4]_2$.** A solution containing 0.58 g (3 mmol) of btzb dissolved in 80 ml of methanol was added to a solution of 0.36 g (1 mmol) $Fe[ClO_4]_2 \cdot 6H_2O$ and 5 mg of ascorbic acid dissolved in 10 ml of methanol. The compound crystallised upon evaporation of the solvent at room temperature after a few days. The colourless crystals were filtered off, washed with ethanol and dried in air. The compound is not sensitive to oxidation upon exposure to the air. Yield 0.33 g, 39% (Calc. for $C_{18}H_{30}Cl_2FeN_{24}O_8$: C, 25.82; H, 3.61; Fe, 6.67; N, 40.15. Found: C, 26.10; H, 3.68; Fe, 6.27; N, 39.44%).

**$[Cu(btzb)_3][ClO_4]_2$ and $[Ni(btzb)_3][ClO_4]_2$.** A solution containing 0.29 g (1.5 mmol) of btzb dissolved in 25 ml of hot water was added to a solution of 0.18 g (0.5 mmol) $Cu[ClO_4]_2 \cdot 6H_2O$ (or $Ni[ClO_4]_2 \cdot 6H_2O$) dissolved in 10 ml of water. The copper(II) compound crystallised in the form of light blue crystals and the nickel(II) one as purple crystals upon evaporation of the solvent at room temperature after a few days. The crystals were filtered off, washed with water and dried in air. Yield for $[Cu(btzb)_3][ClO_4]_2$: 0.22 g, 51% (Calc. for $C_{18}H_{30}Cl_2CuN_{24}O_8$: C, 25.58; H, 3.58; N, 39.78. Found: C, 25.41; H, 3.53; N, 40.08%). Yield for $[Ni(btzb)_3][ClO_4]_2$: 0.10 g, 24% (Calc. for $C_{18}H_{30}Cl_2O_8N_{24}Ni$: C, 25.73; H, 3.60; N, 40.01. Found: C, 25.43; H, 3.58; N, 39.81%).

### X-Ray crystallography

**1,4-Bis(tetrazol-1-yl)butane.** Data were collected on a Enraf-Nonius CAD4 Turbo diffractometer with graphite monochromated Mo-Kα ($\lambda = 0.71073$ Å) radiation and corrected for Lorentz polarisation effects and for a linear instability of 3% of the reference reflections, but not for absorption. The structure was solved by direct methods (SHELXS 96).[17] 84 Parameters (including coordinates for hydrogen and non-hydrogen atoms, anisotropic displacement parameters for non-H atoms and isotropic displacement parameters for hydrogen atoms) were refined on $F^2$ using full-matrix least-squares techniques (SHELXL 97-2).[18] A final Fourier difference map showed no residual density outside −0.33 and 0.28 e $Å^{-3}$. Crystal and diffraction data are listed in Table 1.

CCDC reference number 186/2298.

See http://www.rsc.org/suppdata/dt/b0/b008073j/ for crystallographic files in .cif format.

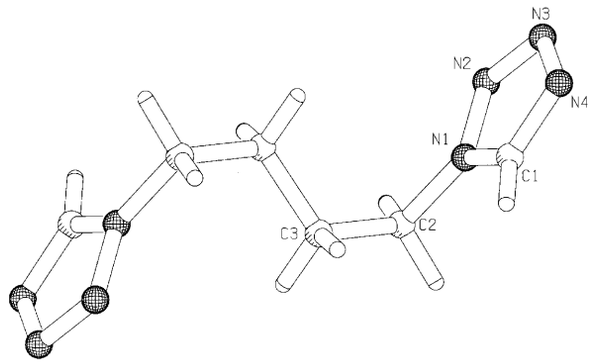


**Fig. 1** PLUTON[19] drawing (50% probability) and atomic labelling system showing the structure of 1,4-bis(tetrazol-1-yl)butane.

**$[Fe(btzb)_3][ClO_4]_2$.** No single crystals suitable for X-ray diffraction could be obtained for $[Fe(btzb)_3][ClO_4]_2$. All attempts resulted in the formation of crystals consisting of multiple individuals severely intergrown. These all displayed diffraction patterns with broad, unstructured streaks, several degrees in width, instead of single Bragg spots. Data collected on them indicated a pseudo-hexagonal unit cell, with $a = 10.754(3)$, $b = 10.768(4)$, $c = 17.43(1)$ Å, $\alpha = 89.47(4)$, $\beta = 88.36(4)$, $\gamma = 60.46(3)°$. Intensity data were collected up to $\theta = 21°$ at 150 K for one of the samples with the smallest streak width (*i.e.* less than 7°). This crystal showed an intensity decay of more than 30% during X-ray exposure. Attempts to apply direct methods and Patterson methods on these data resulted in poor electron density maps. On these maps only the iron position could clearly be identified. The Fourier maps, which were calculated with phase information obtained from the iron position, showed strands of electron density connecting the iron(II) ions. A large number of maxima was found in these strands. A selection of peaks was made on the basis of chemically reasonable distances, neglecting the relative weight of the peaks. From this selection a rough model of the btzb ligand could be made. Refinement of the coordinates of this model showed the atomic positions to be more or less stable at the observed positions. However, the geometric parameters of the ligand showed large deviations (0.2–0.4 Å and 10–20°) from their expected values and are therefore not relevant. In view of the resolution and the low quality of the dataset, introduction of constraints or restraints is not warranted, and the model should only be considered as a rough indication of the position of the ligands. The atoms of the counter anions could be located in channels parallel to the *c* axis in a similar way to the atoms of the bridging ligands.

## Results

### Crystal structure of 1,4-bis(tetrazol-1-yl)butane

A projection of the structure of btzb is given in Fig. 1, whereas relevant bond distances and angles are listed in Table 2. The monoclinic cell contains two btzb molecules. The asymmetric unit contains one half of the btzb molecule with an inversion centre located on the C3–C3′ linkage. The bond lengths and bond angles involving the tetrazole nuclei may be considered as normal.[13,20] Owing to symmetry considerations, the angle between the tetrazole ring planes is 180°. Therefore, free btzb is in the *anti* conformation, which is in contrast to what has been found for [tris(1,2-bis(tetrazol-1-yl)iron(II) bisperchlorate where the ligand is in the *syn* conformation due to the linking of two iron(II) ions using the *N*4 and *N*4′ tetrazole ring atoms.[13] For btzb the deviation of the tetrazole rings from planarity is less than 0.001(1) Å. The crystal packing shows that the crystallographically dependent molecules are oriented in a chain-like arrangement in a head to tail fashion along the *c* axis. These

**Table 1** Crystal and diffraction data for 1,4-bis(tetrazol-1-yl)butane

| | |
|---|---|
| Formula | $C_6H_{10}N_8$ |
| $M$ | 194.2 |
| Crystal system | Monoclinic |
| Space group | $P2_1/c$ (no. 14) |
| $a$/Å | 5.373(1) |
| $b$/Å | 12.481(1) |
| $c$/Å | 7.293(2) |
| $\beta$/° | 114.88(2) |
| $V$/Å$^3$ | 443.7(2) |
| $T$/K | 150 |
| $Z$ | 2 |
| $\mu$(Mo-K$\alpha$)/cm$^{-1}$ | 1.0 |
| Reflections collected | 2345 |
| Independent reflections | 1012 ($R_{int}$ = 0.0483) |
| $R1$ [$I > 2\sigma(I)$], $wR2$, $S$ | 0.345 (883 refl.), 0.0834, 1.122 |

**Table 2** Bond distances (Å) and angles (°) for 1,4-bis(tetrazol-1-yl)-butane

| | | | |
|---|---|---|---|
| N2–N2 | 1.342(2) | N3–N4 | 1.358(1) |
| N1–C1 | 1.331(1) | N4–C1 | 1.314(2) |
| N1–C2 | 1.471(1) | C2–C3 | 1.518(2) |
| N2–N3 | 1.299(2) | C3–C3′ | 1.5223(2) |
| N2–N1–C1 | 108.17(9) | N3–N4–C1 | 104.94(9) |
| N2–N1–C2 | 122.08(9) | N1–C1–N4 | 109.6(1) |
| C1–N1–C2 | 129.8(1) | N1–C2–C3 | 111.14(9) |
| N1–N2–N3 | 106.2(1) | C2–C3–C3′ | 112.5(1) |
| N2–N3–N4 | 111.1(1) | | |

Primed atoms are generated by the symmetry operation $-x, -y, -z$.

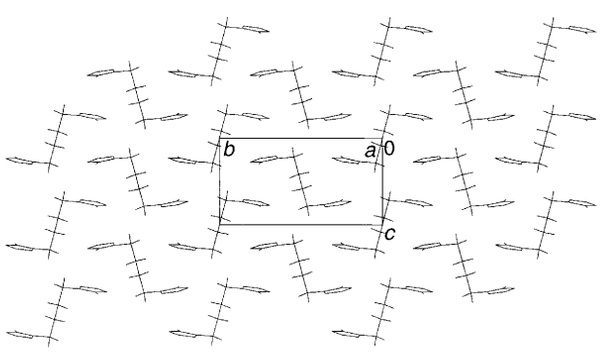


**Fig. 2** PLUTON[19] drawing showing the crystal packing of 1,4-bis(tetrazol-1-yl)butane.

chains are organised in such a way as to form a herringbone motif. The crystal packing shows the tetrazole rings to be ordered in π-stacked columns with interplanar angles of 18°. The distance between the geometrical centres of two stacked rings is 3.73 Å. The butane groups point outwards of these columns in a herringbone like arrangement (see Fig. 2). The structure is further stabilised by a short C1–H · · · N3 interaction, with H · · · N 2.41(2) Å (*i.e.* 0.34 Å shorter than the sum of the van der Waals radii) and C–H · · · N 157(1)°.

### 3-D Model for $[Fe(btzb)_3][ClO_4]_2$

Fig. 3 shows a tentative model of the 3-D structure of $[Fe(btzb)_3][ClO_4]_2$. Each of the ligands is located on an inversion centre (as is also the case in the crystal structure of the "free" ligand). This causes all central C–C linkages to be in the *anti* conformation. Of the six independent N–C–C–C torsions in the ligands, four are also in the *anti* conformation, but two fit the electron density best when brought into a *gauche* conformation. The model shows two symmetry-related, interpenetrating, 3-D Fe–btzb networks. Iron atoms within one network are separated by the unit cell translations. The iron atoms of two non-connected networks approach each other as close as 8.3 and 9.1 Å according to this model.

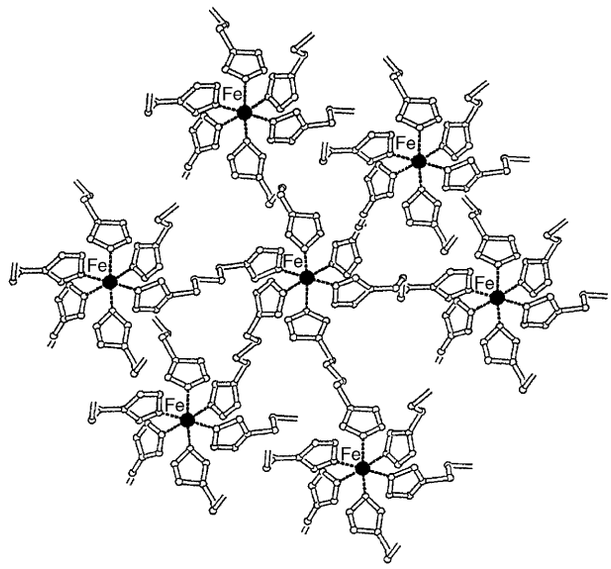


**Fig. 3** PLUTON[19] drawing showing the tentative 3-D model for $[Fe(btzb)_3][ClO_4]_2$.

### Infrared spectroscopy

The series of compounds $[M(btzb)_3][ClO_4]_2$ ($M^{II}$ = Fe, Ni or Cu) have essentially identical infrared spectra. There is no evidence for strong deviation from $T_d$ symmetry for the non-coordinating perchlorate anions, which is consistent with the presence of the strong and broad $\nu_3$ absorption at 1100 cm$^{-1}$ and the $\nu_4$ at 624 cm$^{-1}$, as well as the absence of any sign of the $\nu_1$ absorption.[21]

### EPR spectroscopy

The X-band powder EPR spectrum recorded for $[Cu(btzb)_3][ClO_4]_2$ at 298 K shows a signal at $g = 2.06$ and hyperfine structure ($A_{\|}$ = 148 Gauss), which is typical for an isolated copper(II) ion. In the EPR spectra no indications for Cu · · · Cu exchange splittings are observed.[22]

### Ligand-field spectroscopy

The UV/Vis spectrum for $[Cu(btzb)_3][ClO_4]_2$ shows a broad asymmetric band with a maximum situated at $17.2 \times 10^3$ cm$^{-1}$ and a shoulder at $8.9 \times 10^3$ cm$^{-1}$, which is consistent with the presence of a tetragonally distorted $Cu^{II}N_6$ chromophore.[22]

### Variable temperature optical spectroscopy

$[Fe(btzb)_3][ClO_4]_2$ is obtained as white crystals. This colour arises from the fact that the spin-allowed d–d transition of lowest energy of the compound in the HS state, $^5T_{2g} \longrightarrow {}^5E_g$, occurs at the limit of the visible and IR regions. Upon cooling, the colour changes to an intense pink. This is due to the $^1A_{1g} \longrightarrow {}^1T_{1g}$ d–d transition of the compound in the LS state. Since $[Fe(btzb)_3][ClO_4]_2$ is highly thermochromic the iron(II) spin transition has been studied optically using the device previously described[8,14] which provides an accurate determination of the transition temperatures, but does not give any information on the population of the active SC sites, *i.e.* the percentage of iron(II) ions involved in the spin transition. The results of the optical measurements are displayed in Fig. 4. Upon cooling, a very abrupt HS $\longrightarrow$ LS transition taking place at 155 K is observed. Subsequent heating shows the LS $\longrightarrow$ HS transition at 180 K, yielding a thermal hysteresis of 25 K. Subsequent heating-and-cooling cycles in the temperature range 77–298 K indicate that this hysteresis is retained.

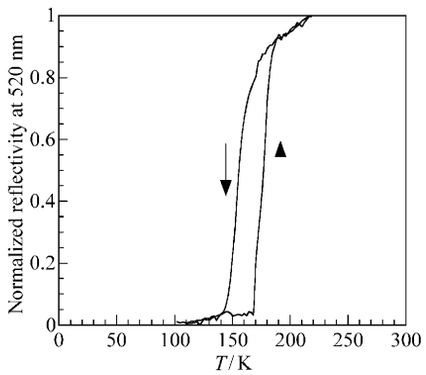


**Fig. 4** Optical detection of the spin transition for $[Fe(btzb)_3][ClO_4]_2$.

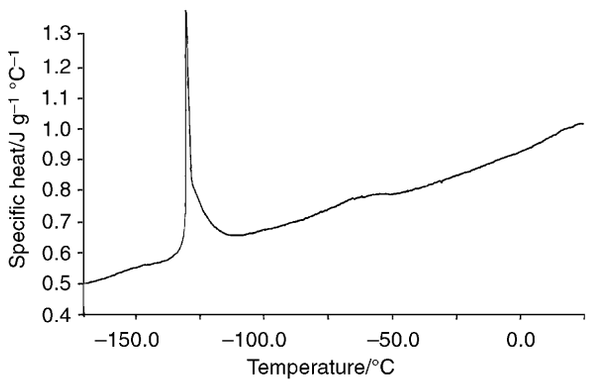


**Fig. 5** Differential Scanning Calorimetry for $[Fe(btzb)_3][ClO_4]_2$ recorded in the heating mode.

### Differential scanning calorimetry

The DSC curve recorded in the cooling mode is displayed in Fig. 5. This curve shows an endothermic peak around 145 K. This very sharp peak is characteristic for a first order transition, and can directly be correlated to the LS ⟶ HS transition detected by optical measurements. The thermodynamic parameters calculated for this spin transition are: $\Delta H = 2.35$ kJ mol$^{-1}$ and $\Delta S = 16.29$ J K$^{-1}$ mol$^{-1}$. DSC experiments carried out on samples previously measured and aged for seven months did not reveal any peaks.

### Magnetic properties

Magnetic data for a freshly prepared sample of $[Fe(btzb)_3][ClO_4]_2$ have been recorded in the temperature range 4.2–298 K (see Fig. 6). At room temperature, $\chi_m T$ is equal to 3.42 cm$^3$ K mol$^{-1}$, which is within the range of values expected for a HS iron(II) ion. As the temperature is lowered, $\chi_m T$ first remains constant then rapidly decreases around 150 K to a value of 2.85 cm$^3$ K mol$^{-1}$, after which it remains constant, and rapidly decreases to 2.6 cm$^3$ K mol$^{-1}$ down to 4.2 K. As the temperature is increased a sharp LS ⟶ HS transition is observed around 170 K revealing a thermal hysteresis of 20 K. This hysteresis has been reproduced along several thermal cycles. It is worth mentioning that the spin transition is not complete, only *ca.* 16% of active iron(II) sites being concerned by the thermal SC. The slight discrepancy between the transition temperatures determined by optical and magnetic methods is most likely related to different sample–thermal response/temperature detector geometries in both applied techniques. The optical measurements focus on the colour, *i.e.* the surface of the sample, whereas the magnetic data reflect the physical behaviour of the bulk material.[23]

### LIESST experiment

$[Fe(btzb)_3][ClO_4]_2$ was slowly cooled to 30 K within a SQUID cavity. Irradiation with green light affords a dramatic increase of the magnetic moment evidencing a light induced population LS ⟶ HS (LIESST effect).[24] About 15% of LS iron(II) ions were involved in the optical switching. Upon heating, thermal relaxation occurs from the metastable HS state back to the LS state in the 40–60 K temperature range.

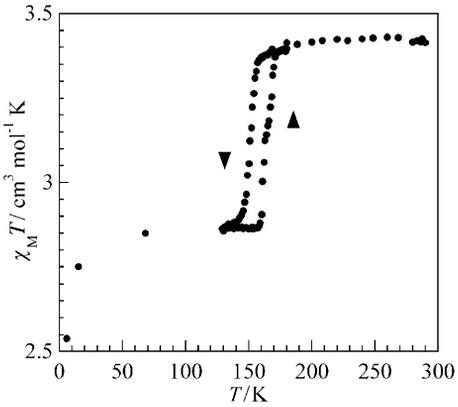


**Fig. 6** $\chi_m T$ *vs.* $T$ curve for $[Fe(btzb)_3][ClO_4]_2$.

### $^{57}$Fe Mössbauer spectroscopy

$^{57}$Fe Mössbauer spectra for $[Fe(btzb)_3][ClO_4]_2$ have been recorded in the heating mode at various temperatures between 77 and 230 K. Selected spectra are depicted in Fig. 7 and the corresponding Mössbauer parameters are given in Table 3. At 77 K the spectrum shows a major doublet (spectral contribution of 94.4%) with an isomer shift of 1.16(1) mm s$^{-1}$ and a large quadrupole splitting of 2.37(1) mm s$^{-1}$, which may be attributed to iron(II) ions in the HS state. The minor contribution (*ca.* 5.6%) yields an isomer shift value of 0.54(1) mm s$^{-1}$ with a negligible quadrupole splitting. Such LS iron(II) singlet spectra have been reported for $[Fe(ptz)_6][BF_4]_2$ (ptz = 1-propyltetrazole), where the absence of any splitting could be related to one of the rare cases of quasi cubic local symmetry.[25] Upon heating, *ca.* 5% of iron(II) ions in LS state convert into the HS state. At 175 K the spectrum uniquely consists of HS iron(II) characterised by an isomer shift $\delta$ of 1.11(1) mm s$^{-1}$ and a quadrupole splitting of 2.08(2) mm s$^{-1}$. The transition temperature found in the heating mode (*ca.* 168 K) matches the one found by magnetic measurements.

## Discussion

### Structural aspects

The present series of infrared isomorphous coordination compounds $[M(btzb)_3][ClO_4]_2$ ($M^{II}$ = Fe, Ni or Cu) have a polynuclear structure. It is well known that 1-alkyl-substituted tetrazoles yield mononuclear octahedrally surrounded transition metal(II) compounds, in which six tetrazole ligands coordinate monodentately to the metal ion by N4.[6,20,25–34] Recently, the same coordination mode of the tetrazole nucleus has been found for [tris(1,2-bis(tetrazol-1-yl)propane)iron(II) bisperchlorate yielding a 1-D compound,[13] in which three ligands in *syn* conformation link the iron(II) ions *via* N4 and N4′. The crystal structure of btzb has revealed that it favours an *anti* conformation. Unfortunately, the spectroscopic studies do not allow any predictions concerning the conformation of the btzb ligand in the present coordination compounds. However, it appears that in $[Fe(btzb)_3][ClO_4]_2$ four of the six crystallographically independent btzb ligands are in an *anti* conformation, whereas the remaining two are in a *syn* conformation.

Studies on polynuclear transition metal(II) compounds of bis(1,2,4-triazol-1-yl)[35] and bis(1,2,4-triazol-4-yl)[36] with alkyl spacers have shown that upon increasing length of the spacer

**Table 3** $^{57}$Fe Mössbauer parameters (in mm s$^{-1}$) for $[Fe(btzb)_3][ClO_4]_2$[a] recorded in the heating mode

| $T$/K | $\delta$ (LS) | $\Delta E_Q$ (LS) | $\Gamma$ (LS) | $\delta$ (HS) | $\Delta E_Q$ (HS) | $\Gamma$ (HS) | $A_{HS}$(%) |
|---|---|---|---|---|---|---|---|
| 77 | 0.54(1) | *0* | 0.26(2) | 1.16(1) | 2.37(1) | *0.344* | 94.4 |
| 120 | 0.51(1) | *0* | *0.26* | 1.13(1) | 2.26(2) | *0.344* | 96.3 |
| 145 | 0.49(1) | *0* | *0.26* | 1.12(1) | 2.19(2) | *0.344* | 96.0 |
| 160 | 0.51(1) | *0* | *0.26* | 1.15(1) | 2.14(2) | *0.344* | 96.4 |
| 166 | 0.50(1) | *0* | *0.26* | 1.14(1) | 2.12(3) | *0.344* | 96.5 |
| 170 | 0.49(1) | *0* | *0.26* | 1.11(1) | 2.10(3) | *0.344* | 98.4 |
| 175 | — | — | — | 1.11(1) | 2.08(2) | *0.344* | 100 |
| 178 | — | — | — | 1.11(1) | 2.07(2) | *0.344* | 100 |
| 230 | — | — | — | 1.08(1) | 1.85(3) | 0.344(4) | 100 |

[a] $\delta$ = Isomer shift relative to iron metal at 295 K, $\Delta E_Q$ = quadrupole splitting, $\Gamma$ = Lorentzian linewidth, $A_{HS}$ = relative area of the HS doublets. Statistical standard deviations are given in parentheses. Values in italics were fixed during the fit.

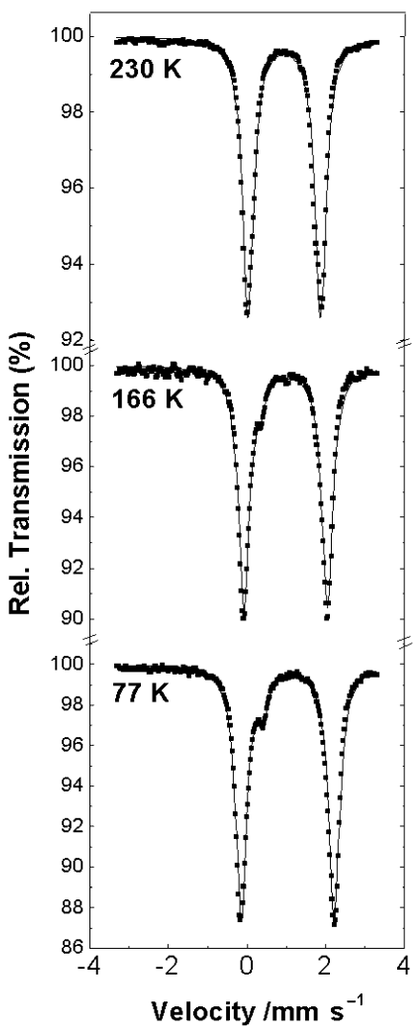


**Fig. 7** Selected $^{57}$Fe Mössbauer spectra for $[Fe(btzb)_3][ClO_4]_2$ recorded in the heating mode.

the ligands tend to link several metal(II) ions, thereby yielding 3-D supramolecular compounds. This may be governed by the fact that upon increasing spacer length the *anti* conformation as has been found for free btzb is favoured over the bent *syn* conformation as found in coordination compounds of ligands with smaller spacers. It may be proposed that the increase in length from 1,2-propane to 1,4-butane in the present bis(tetrazole) ligands will follow these rules, yielding 3-D btzb coordination compounds. $[Fe(btzb)_3][ClO_4]_2$ represents actually a molecular SC catenane with a 3-D network. The first supramolecular 2-D catenane exhibiting thermal SC behaviour was found for [bis(1,2-di(4-pyridyl)ethylene)dithiocyanatoiron(II)][37] whereas $[Fe(btr)_3][ClO_4]_2$ (btr = 4,4′-bis-1,2,4-triazole) represents the first SC compound with a 3-D network.[38]

The EPR spectroscopy data on $[Cu(btzb)_3][ClO_4]_2$ have shown that no Cu · · · Cu exchange splittings could be detected and the EPR signal corresponds to what could be expected for isolated copper(II) ions. From these results it may be that the Cu · · · Cu separations in this compound are rather large, which is also supported by the Fe · · · Fe spacings of 8.3 and 9.1 Å estimated for $[Fe(btzb)_3][ClO_4]_2$.

### Spin transition features of $[Fe(btzb)_3][ClO_4]_2$

It is well known that 1-alkyl-substituted tetrazoles yield mononuclear iron(II) SC compounds.[6,20,25–34] Although all iron(II) ions are also surrounded by six N-donating tetrazole moieties in the present $[Fe(btzb)_3][ClO_4]_2$, the magnetic behaviour is somewhat different. On the one hand the spin transition is accompanied by a pronounced thermochromic effect and takes place in a very abrupt fashion with a thermal hysteresis of 20 K. The transition temperatures were estimated as $T_{1/2}\uparrow$ = 170 K and $T_{1/2}\downarrow$ = 150 K as determined from variable temperature magnetic susceptibility measurements. This is the largest thermal hysteresis observed up to now for iron(II) tetrazole derivatives. On the other hand, the magnetic and $^{57}$Fe Mössbauer data show that a small fraction of iron(II) ions is involved in the SC process down to very low temperatures. This explain the unusually low values of the enthalpy and entropy variations associated with the spin transition. This retention of the HS state may not be explained by spin freezing, as has been observed for instance for [$Fe^{II}$-(3-MeO,5-$NO_2$-sal-N(1,10)-NMe(4,7))],[39] since for the present compound the LS–HS relaxation appears to be rather fast at the transition temperature. This is confirmed by the fact that slow cooling of the sample during the $^{57}$Fe Mössbauer measurements did not lead to an increase of the LS fraction.

The occurrence of a sharp transition with a wide hysteresis is hardly conceivable for a system for which only a small fraction of active SC sites is present. Indeed such a high degree of dilution should have weakened the co-operativity so as completely to smooth the spin transition. Furthermore, the measured width of the thermal hysteresis loop does not sizeably depend on the ratio of active SC sites, which obviously decreases experiment after experiment. These features strongly suggest a biphasic character for the structural state of the samples. This has been confirmed by a further investigation of the samples after aging for several months, as no thermal SC behaviour could be observed as evidenced by DSC, optical, magnetic measurements and Mössbauer spectroscopy. This behaviour may be explained by progressive loss of a small amount of solvent molecules (water or methanol, which could not be detected by elemental analyses). This transformation induces a switching of the crystallites from a SC active phase to a slightly different one, thermally SC inactive. This latter phase which uniquely contains HS iron(II) ions is currently the subject of extensive photo-magnetic studies in our laboratories.[40] Such aging effects have been observed previously,[41] the closest example being found for the 2-D spin transition compound $[Fe(btr)_2(NCS)_2]\cdot H_2O$,[42] where the hydrate displays thermal

SC behaviour whereas the dehydrated sample remains in the HS state over the whole temperature range.

## Conclusion

$[Fe(btzb)_3][ClO_4]_2$ represents a supramolecular catenane SC compound with a 3-D network. This system can be switched by both temperature and light. The spin transition is surprisingly highly co-operative with respect to the relatively small amount of iron(II) ions concerned by the switching process. The situation is attributed to the progressive loss of solvent molecules, which progressively transforms the SC active crystallites into SC inactive ones. The aged sample of $[Fe(btzb)_3][ClO_4]_2$ represents the first example of a hexakis(1-alkyltetrazole) iron(II) chromophore that does not display thermal SC.

## Acknowledgements

This work was partly funded by the TMR Research Network under contract number ERB-FMRX-CT98-0199, by the Netherlands Foundation of Chemical Research (SON) and by the Netherlands Organisation for Scientific Research (NWO). We thank L. Rabardel for recording the DSC data and A. Goujon for his assistance.

## References

1 O. Kahn and J. P. Launay, *Chemtronics*, 1988, **3**, 140.
2 P. Gütlich, *Struct. Bonding* (*Berlin*), 1981, **44**, 83.
3 J. Zarembowitch and O. Kahn, *New J. Chem.*, 1991, **15**, 181.
4 E. König, *Prog. Inorg. Chem.*, 1987, **35**, 527.
5 J. G. Haasnoot, in *Magnetism: A Supramolecular Function*, ed. O. Kahn, Kluwer Academic Publishers, Dordrecht, 1996, 299.
6 P. Gütlich, A. Hauser and H. Spiering, *Angew. Chem.*, *Int. Ed. Engl.*, 1994, **33**, 2024.
7 P. Gütlich, Y. Garcia and H. A. Goodwin, *Chem. Soc. Rev.*, 2000, **29**, 419.
8 O. Kahn and E. Codjovi, *Philos. Trans. R. Soc. London*, *Ser. A*, 1996, **354**, 359.
9 O. Kahn and C. Jay-Martinez, *Science*, 1998, **279**, 44.
10 O. Kahn, E. Codjovi, Y. Garcia, P. J. van Koningsbruggen, R. Lapouyade and L. Sommier, in Molecule-Based Magnetic Materials, (eds. M. M. Turnbull, T. Sugimoto and L. K. Thompson), *ACS Symp. Ser.*, 1996, **644**, 298.
11 O. Kahn, J. Kröber and C. Jay, *Adv. Mater.*, 1992, **4**, 718.
12 C. Jay, F. Grolière, O. Kahn and J. Kröber, *Mol. Cryst. Liq. Cryst.*, 1993, **234**, 255.
13 P. J. van Koningsbruggen, Y. Garcia, O. Kahn, L. Fournès, H. Kooijman, J. G. Haasnoot, J. Moscovici, K. Provost, A. Michalowicz, F. Renz and P. Gütlich, *Inorg. Chem.*, 2000, **39**, 1891.
14 E. Codjovi, L. Sommier, O. Kahn and C. Jay, *New J. Chem.*, 1996, **20**, 503.
15 Y. Garcia, P. J. van Koningsbruggen, R. Lapouyade, L. Fournès, L. Rabardel, O. Kahn, V. Ksenofontov, G. Levchenko and P. Gütlich, *Chem. Mater.*, 1998, **10**, 2426.
16 T. Kamiya and Y. Saito, *Ger. Offen.*, 2147023, 1973.
17 G. M. Sheldrick, SHELXS 96, Program for crystal structure determination, University of Göttingen, 1996.
18 G. M. Sheldrick, SHELXL 97-2, Program for crystal structure refinement, University of Göttingen, 1997.
19 A. L. Spek, *Acta Crystallogr.*, *Sect. A*, 1990, **46**, C-34.
20 L. Wiehl, *Acta Crystallogr.*, *Sect. B*, 1993, **49**, 289.
21 K. Nakamoto, *Infrared and Raman Spectra of Inorganic and Coordination Compounds*, 3rd edn., Wiley, New York, 1978.
22 B. J. Hathaway and D. E. Billing, *Coord. Chem. Rev.*, 1970, **5**, 143.
23 F. Varret, H. Constant-Machado, J. L. Dormann, A. Goujon, J. Jeftic, M. Noguès, A. Bousseksou, S. Klokishner, A. Dolbecq and M. Verdaguer, *Hyperfine Interact.*, 1998, **113**, 37; W. Morscheidt, E. Codjovi, J. Jeftic, J. Linarès, A. Bousseksou, H. Constant-Machado and F. Varret, *Meas. Sci. Technol.*, 1998, **9**, 1311; E. Codjovi, W. Morscheidt, J. Jeftic, J. Linares, M. Nogues, A. Goujon, O. Roubeau, H. Constant-Machado, A. Desaix, A. Bousseksou, M. Verdaguer and F. Varret, *Mol. Cryst. Liq. Cryst.*, 1999, **335**, 1295.
24 S. Decurtins, P. Gütlich, C. P. Köhler, H. Spiering and A. Hauser, *Chem. Phys. Lett.*, 1984, **1**, 139; S. Decurtins, P. Gütlich, K. M. Hasselbach, H. Spiering and A. Hauser, *Inorg. Chem.*, 1985, **24**, 2174.
25 P. L. Franke, J. G. Haasnoot and A. P. Zuur, *Inorg. Chim. Acta*, 1982, **59**, 5.
26 E. W. Müller, J. Ensling, H. Spiering and P. Gütlich, *Inorg. Chem.*, 1983, **22**, 2074.
27 P. Poganiuch and P. Gütlich, *Hyperfine Interact.*, 1988, **40**, 331.
28 P. Adler, P. Poganiuch and H. Spiering, *Hyperfine Interact.*, 1989, **52**, 47.
29 P. Poganiuch, S. Decurtins and P. Gütlich, *J. Am. Chem. Soc.*, 1990, **112**, 3270.
30 P. Gütlich and P. Poganiuch, *Angew. Chem.*, *Int. Ed. Engl.*, 1991, **30**, 975.
31 T. Buchen and P. Gütlich, *Chem. Phys. Lett.*, 1994, **220**, 262.
32 T. Buchen, P. Poganiuch and P. Gütlich, *J. Chem. Soc.*, *Dalton Trans.*, 1994, 2285.
33 R. Hinek, H. Spiering, D. Schollmeyer, P. Gütlich and A. Hauser, *Chem. Eur. J.* 1996, **2**, 1127.
34 J. Jeftic, R. Hinek, S. C. Capelli and A. Hauser, *Inorg. Chem.*, 1997, **36**, 3080.
35 J. G. Haasnoot, *Coord. Chem. Rev.*, 2000, **200**–**202**, 131.
36 Y. Garcia, P. J. van Koningsbruggen, H. Kooijman, A. L. Spek, J. G. Haasnoot and O. Kahn, *Eur. J. Inorg. Chem.*, 2000, 307; Y. Garcia, P. J. van Koningsbruggen, H. Kooijman, A. L. Spek, J. G. Haasnoot and O. Kahn, *Eur. J. Inorg. Chem.*, 2000, 575.
37 J. A. Real, E. Andrés, M. C. Munoz, M. Julve, T. Granier, A. Bousseksou and F. Varret, *Science*, 1995, **268**, 265.
38 Y. Garcia, O. Kahn, L. Rabardel, B. Chansou, L. Salmon and J.-P. Tuchagues, *Inorg. Chem.*, 1999, **38**, 4663.
39 A. Bousseksou, L. Salmon, F. Varret and J.-P. Tuchagues, *Chem. Phys. Lett.*, 1998, **282**, 209.
40 A. Goujon, Y. Garcia, J. Linares and F. Varret, in preparation.
41 D. C. Craig, H. A. Goodwin, D. Onggo and A. D. Rae, *Aust. J. Chem.*, 1988, **41**, 1265; K. H. Sugiyarto and H. A. Goodwin, *Aust. J. Chem.*, 1994, **47**, 263.
42 W. Vreugdenhil, J. H. van Diemen, R. A. G. de Graaff, J. G. Haasnoot, J. Reedijk, A. M. van der Kraan, O. Kahn and J. Zarembowitch, *Polyhedron*, 1990, **9**, 2971.